Study of Thermo-Mechanical Damage around Deep Geothermal Wells: from the Micro-Processes to Macroscopic Effects in the Near Well

Mariane Peter-Borie, Arnold Blaisonneau, Sylvie Gentier, Théophile Guillon, Xavier Rachez

Proceedings World Geothermal Congress 2015
Melbourne, Australia, 19-25 April 2015

Study of Thermo-Mechanical Damage around Deep Geothermal Wells: from the Micro-Processes to Macroscopic Effects in the Near Well

Mariane Peter-Borie, Arnold Blaisonneau, Sylvie Gentier, Théophile Guillon, Xavier Rachez

BRGM DGR/DES - 3, av. C. Guillemin, BP 36009 - 45060 Orléans cedex 2, FRANCE

m.peter@brgm.fr

Keywords: bonded particle model, breakout, deep geothermal well, DEM, granite, induced tensile fractures, Melleray, near well, PFC, sandstone, Soultz, thermo-mechanical damage

ABSTRACT

The different processes involved in the life of a geothermal well, from drilling to exploitation, can damage the rock mass in the near well area. In this paper, we propose to study the potential damage linked to the mechanical and thermo-mechanical effects of the well drilling, the well development and the well exploitation. The cooling of the rock mass of the near well pre-damaged by drilling process is a complex phenomenon with the superimposition of different kind of loadings at different scale that lead us to use modeling with a micro-macro approach. To confront the results of the modeling with the reality, we propose to base our study on real cases. For studying mechanical and thermo-mechanical loadings due to drilling and development of the well, we focus our study on the granitic reservoir exploited in the framework of the enhanced geothermal system (EGS) of Soultz-sous-Forêts (France). The study of the thermo-mechanical loading due to well exploitation is performed for a sandstone in the conventional heat exploitation of Melleray (Loiret, France). These simulations highlight the thermo-mechanical damage of a geothermal well linked to the different steps of its life.

1. INTRODUCTION

Numerous references to damaging of well walls under mechanical and thermo-mechanical solicitations can be found in the literature, particularly in the context of oil extraction. For a long time now, this phenomenon has been classically studied to determine the stress state by analyzing the shape of breakouts and of drilling-induced tensile fractures (*e.g.* Bell and Gough, 1979, Zoback et al., 1985, Stephens and Voight, 1982). In sandstones, it can lead to sand production problems ("sanding", *e.g.* Morita and Boyd, 1991). Similar damaging is observed in deep geothermal wells: for example in Soultz-sous-Forêts enhanced geothermal system, ultrasonic borehole imager performed after drilling operation show breakouts and induced fractures (Bérard, 2003, Valley and Evans, 2006); in Melleray deep geothermal exploitation, a large phenomenon of sanding occurred in the injection well (Boisdet et al., 1989). In order to have a better understanding of these phenomena in deep geothermal wells, and bearing in mind the aim of optimizing the reservoir connection to the well and to limit the rock pervasive damaging, we propose to study the effects of mechanical and thermo-mechanical loadings associated with the drillings, well development and exploitation.

The complexity and the superimposition of the physical processes involved in these operations lead us to have a numerical modeling approach. The numerical method is chosen according to the physical processes we wish to study. The thermal solicitation induces differential strains at the origin of thermo-mechanical stresses. When these stresses exceed the mechanical resistance of the rock, microcracks and failures can appear. Strains at the origin of this process can be mainly due to two causes: on the one hand a difference of temperature in the rock mass, on the other hand the heterogeneity of the grains contraction in the rock. Because of this heterogeneity, two adjacent mineral phases can contract at different rate and thus generate uneven strains at the grain boundaries (Wanne and Young, 2008). Discrete Element Method (DEM) based on the micro-macro approach looks fairly adapted to catch these thermo-mechanical processes. The DEM allows to take into account the physical phenomena at the granular phase level (micro scale), as well as their impact on the mechanical behavior of the near well zone (macro scale).

After a brief presentation of the DEM used in our work, this paper first deals with how the rocks involved in the studied cases are modeled as assemblies of bonded particles. It then presents the results of the modeling of the well drilling, the well development and the well exploitation.

2. NUMERICAL APPROACH: BONDED PARTICLE MODEL

Bonded particle models are carried out with the PFC2D code (© Itasca), whose principle is the modeling of the movement and interaction of the non-uniform-sized circular particles using discrete element method (DEM Cundall, 1971). The definition of the microscopic parameters, *i.e.* particles and bonds geometrical, physical, mechanical and thermo-mechanical characteristics, is crucial to reproduce the behavior of the rock at a macro scale (Potyondy and Cundall, 2004). After a brief presentation of the used DEM, this section mainly deals with the building of the bonded particle model for rocks with grained structure such as granite or sandstone.

2.1 Discrete element method

PFC2D models simulate the movement and interaction of stressed assemblies of rigid circular particles using the Distinct Element Method (DEM). The model is composed of non-uniform-sized distinct particles that displace independently from one another, and interact only at contacts or interfaces between them (Itasca, 2008a). The behavior of the contacts is characterized using a soft contact approach, wherein the particles are allowed to overlap one another at contact points (magnitude of the overlap is related to the contact force via the force-displacement law, and all overlaps are small in relation to particle sizes). Bonds can exist at contacts between particles. The mechanical behavior of such a system is described in terms of the movement of each particle and the inter-particle forces acting at each contact point (figure 1; Itasca, 2008a). In the modeling cases presented in this paper, the particles are

initially bound by a contact Parallel Bond (PB). The macroscopic behavior of the model is governed by the density of the arrangement of the particles, their size distribution and particle properties and contacts (Potyondy and Cundall, 2004).

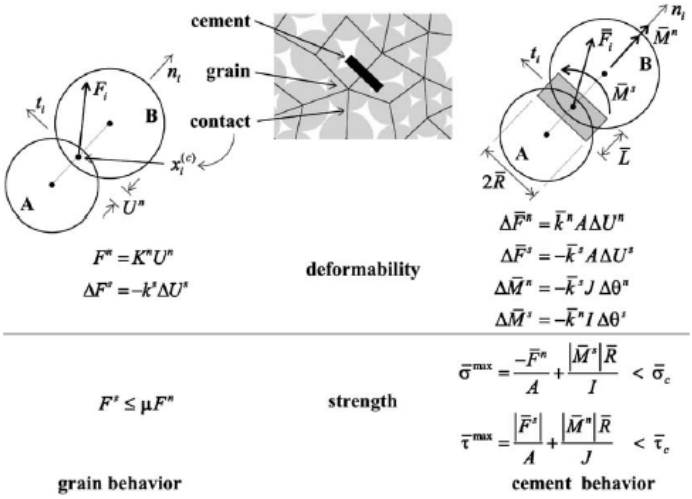

Figure 1: Force–displacement behavior of the particles (grain behavior) and of the parallel bonds (cement behavior; Potyondy and Cundall, 2004)

The thermal capabilities of PFC allow the simulation of transient heat conduction and storage, with each particle being seen as a heat reservoir. For each particle, the temperature value changes with respect of its own specific heat coefficient and thanks to a thermal pipe at each contact with the neighboring particles, if the two particles at the contact are overlapping or if a bond is present (active contact); a pipe length and thermal resistance are assigned to each active contact. When a thermal pipe exists between two particles of two different temperatures, a heat flux takes place in the thermal pipe. Due to their temperature evolutions, a volumetric response (contraction/dilation) of the particles is induced by the integration of radii increment, depending on their respective thermal expansion (Itasca, 2008b). All these thermal volumetric strains are at the origin of a new mechanical equilibrium of the whole model and so of a new stress/strain state. When the model is composed by numerous particles (from about half a million particles), this thermo-mechanical coupling requires a prohibitive computational time. In that case, a one-way coupling only is taken into account to capture the effect of temperature on the mechanical behavior: a homogeneous analytical solution gives the temperature fields, which are then patched on the numerical model particles.

2.2 Bonded particle rock models

The first step of the bonded particle rock building deals with the conceptualization of the real rock. This step is important as it defines the scale of the discretization of the rock according to the scale of the physical phenomenon involved in the problem we have to solve. The particles of the numerical model can represent either the grains of a grained-structured rock, either a homogenized volume of rock (that should be representative within the meaning of representative volume element (RVE) concept). In the problem involved in the studied cases in this paper, a part of the strain generated by the thermal loading applied to the rock mass occurs because of the heterogeneous thermo-mechanical behavior of the mineral phases. The scale of the involved physical phenomena in the studied problem leads to discretizing the sandstone and the granite at the grain scale. The correspondence of the different mineral phases of the rocks with the numerical elements is performed according to their role in the behavior of the rock (Peter-Borie et al. 2011 & 2014): while the particles are predominantly associated with the elastic properties (*e.g.*, Young's modulus) and volumetric characteristics (density) of the material, contacts are mainly associated to the failure. Thus, the mineral phases that compose the granular phases of the sedimentary rocks or the crystals of plutonic rocks, are represented by particles. The contacts between the grains or crystals (for sedimentary rocks: grain-to-grain contacts or grain-to-cement-to-grain contacts, for plutonic rocks: crystal joints) are modeled by Parallel Bonds (PB) as this kind of bond approximates the mechanical behavior of brittle elastic cements. The choice of relative value of PB radius (defined as the PB length reported to the particles diameter and expressed between 0 and 1) should be estimated according to observations of rock thin sections. It could be different for the various kinds of contact (grain-to-grain or grain-to-cement-to-grain contact) for a same sedimentary rock. For plutonic rocks, the crystals are completely jointed by rock fabric processes. However, in specific cases such as hydrothermal alteration, we can make the assumption that the degree of interlocking of crystals decrease locally because of dissolution processes. In this case, the PB length should be also reduced.

2.2.2 Granite bonded particle model

The Soultz granite is a Hercynian monzogranite characterized by phenocrystals of alkali-feldspars in a matrix of quartz, plagioclase, biotite and minor amphibole. In the studied areas, this rock has been hydrothermally altered. As a consequence, most of the plagioclase has been altered in clay. Following the conceptualization methodology, all of the mineral phases will be modeled by particles. Each particle family has the concentration and the crystal size distribution characterizing the corresponding mineral phase in the rocks and that have been determined by image analyses of rocks section by Riss et al. (2001). The table 1 summarizes these data. In this bonded-particle model of the hydrothermally altered granite, we assume that 85% of the grains joint have been altered. The length of PB modeling such altered joint is considered to be equal to 99% of the diameter of the smallest particle of the couple of bonded particles.

Mineral phases	alkali-feldspars	Altered plagioclases/clay	biotite and minor amphibole	Quartz
Concentration	22%	39%	7%	32%
Minimal radius (m)	$3.0\ 10^{-3}$	$2.0\ 10^{-3}$	$1.0\ 10^{-3}$	$1.5\ 10^{-3}$
Maximal radius (m)	$12.0\ 10^{-3}$	$6.0\ 10^{-3}$	$2.0\ 10^{-3}$	$3.5\ 10^{-3}$
Young modulus (MPa)	53	30	72	65

Table 1: Composition of the hydrothermally altered granite of Soultz and properties of the particles modeling the crystals

At the particle scale (micro scale), the properties must be physically consistent with the mineral phase characteristics, and must enable the model to reproduce the macroscopic mechanical and thermo-mechanical behavior of the rock (macro scale). In this way, the mechanical properties of the particles are chosen consistent with the mineral phase of the crystal it models (see table 1 for Young Modulus of each mineral phase). The elastic properties of each PB are equal to the average of elastic properties of the two adjacent particles that constitute the bond. The bonds strengths are defined by the friction angle, cohesion and normal strength in table 2. We can note that the altered crystal joint is characterized by a cohesion slightly lower than that of the non-altered joint.

	Friction angle	Cohesion (MPa - mean value)	Normal strength (MPa - mean value)
Crystal joint	40	270	127
Altered crystal joint	40	267	126

Table 2: Mechanical microproperties of parallel bonds for the granite bonded particle model (mean values for a bond between two particles modeling quartz crystals)

The resulting macroproperties, estimated through simulations of uniaxial and triaxial tests on bonded particles rocks model, are presented in table 3. The macroproperties of the particles assembly and associated bonds are globally those, theoretically estimated by Gentier et al. (2002).

	Granite bonded particle model	Theoretical properties of the hydrothermally altered granite from Gentier et al. (2002)
Unconfined compressive strength (MPa)	128	
Cohesion (MPa)	33.5	34.0
Friction angle (°)	39.2	40.0
Young modulus (GPa)	33.4	32.7

Table 3: Properties of the bonded particles granite model and of the theoretical properties of the hydrothermally altered granite (from Gentier et al., 2002)

2.2.3 Sandstone bonded particle model

The clastic rock involved in the conventional heat exploitation of Melleray is a Triassic sandstone. Few data is available for this specific facies involved in the Melleray well. In this paper, we focus on the sandstone called white sandstone with dolomitic cement. From textural definition (from Cautru and Robelin, 1984), we know that it is a quartzarenite packstone to grainstone with low content of feldspars grains and few lithic fragments contents. The grain size distribution is known heterometric around a min value of $100\ 10^{-6}$ m. For cementing the grain, a major dolomitic cement, lower kaolinite cement and few quartz overgrowth are also noticed. Following the definition of the quartzarenite (*i.e.* composed of greater than 90% detrital quartz) and the packstone to grainstone concept (frame grain supported), we make the assumption that the quartz concentration in the rock is about 95%, feldspars concentration about 4% and lithic fragments concentration about 1%. These rates are reported for particle family and a grain size distribution for the particle is chosen uniform and heterometric between a minimum radius of $50\ 10^{-6}$ m and $1\ 10^{-3}$ m (table 4). The PB are considered to model mainly grain-dolomitic cement-grain contacts (60%), then grain-clayey cement-grain contacts (30%) and finally grain-grain contacts (10%). The rock structure defined as packstone to grainstone associated with a porosity of 10% leads to using a mean value of PB length of 94% of the diameter of the smallest particle of the couple of bonded particles (table 5).

Mineral phases	feldspars	Lithic fragments	Quartz
Concentration	4%	1%	95%
Minimal radius (m)	$0.05\ 10^{-3}$	$0.05\ 10^{-3}$	$0.05\ 10^{-3}$
Maximal radius (m)	$1.0\ 10^{-3}$	$1.0\ 10^{-3}$	$1.0\ 10^{-3}$
Young modulus (MPa)	30	25	60

Table 4: Composition of the sandstones and properties of the particles modeling the grains

The microproperties of particles in the sandstone (table 4) model are based on those used for the granite model: they should be physically consistent with the mineral phase characteristics. The quartz particles Young's modulus is slightly lower in the sandstone than in the granite: it is equal to 60 GPa (65 GPa in the granite). For the Feldspars, the Young's moduli of the alkali and of the altered plagioclases in the granite are respectively 53 GPa and 30 GPa. A value of 30 GPa, equal to those of the altered plagioclase in granite, have been chosen for the feldspars in sandstone to take into account the weathering of this mineral during the transport phase of the sedimentary process.

The petrofabric differences between granite and sandstone are mainly in the grains joint characteristics and properties. In the case of granite, the cooling and solidification of magma with mineral crystallization results in strong joints between crystals. The sandstone is the result of cementation of pre-compacted grains that creates globally weaker links between grains. The three models of sandstone, called G2, G2a and G2b from the strongest to the weakest model, have been built to create different levels of sandstone strength under shear and tensile stress. The table 5 synthetizes the used microproperties and the table 6, the resulting

macroproperties estimated by modeling uniaxial and triaxial tests on bonded particles sandstone models. From G2 to G2a, the cohesion values of the bonds have been reduced – the contacts normal strength remains the same (table 2). It results in a decrease of the unconfined compressive strength and of the cohesion of the rock at macroscale. From G2 to G2b, both the cohesion values and the contacts normal strength have been reduced. It results in a decrease of the unconfined compressive strength, of the cohesion and of the Young modulus of the rock at macroscale.

		PB proportion	Friction angle	Cohesion (MPa - mean value)	Normal strength (MPa - mean value)
Quartz grain-dolomitic cement-quartz grain	G2	60%	38.5	74	20
	G2a		38.5	37	20
	G2b		38.5	19	11
Quartz grain-clayey cement-quartz grain	G2	30%	38.5	68	19
	G2a		38.5	34	19
	G2b		38.5	17	10
Quartz grain-quartz grain	G2	10%	38.5	90	25
	G2a		38.5	45	25
	G2b		38.5	23	13

Table 5: Mechanical microproperties of parallel bonds for the sandstone bonded particle models (mean values for a bond between two particles modeling quartz crystals)

	Sandstone models		
	G2	G2a	G2b
Unconfined compressive strength (MPa)	59	48	29
Cohesion (MPa)	19	15	7
Friction angle (°)	41	39	41
Young modulus (GPa)	40	39	22

Table 6: Properties of the bonded particles sandstone models

3. STUDY OF MECHANICAL AND THERMO-MECHANICAL DAMAGE AROUND DEEP GEOTHERMAL WELL

The effects of drillings, well development and exploitation on the near well area are studied by modeling the corresponding mechanical and thermo-mechanical loadings on the rock modeled with the bonded-particle approach. Simulations are based on two real cases in order to compare and to discuss their results. The study of the impacts of drillings and development of the well is based on the case of the enhanced geothermal system of Soultz-sous-Forêts where data is available thanks to well loggings. The effects of geothermal exploitation (fluid injection) are treated in the case of Melleray where an important sanding phenomenon has been observed after injection tests (Boisdet et al., 1989). Prior to the simulation of a cold fluid injection, the mechanical loading resulting from the well drilling is modeled, as it is a starting point of any operation in a well.

3.2 Drilling and development of a well: case of Soultz-sous-Forêts

The Soultz EGS site is organized around three main deep boreholes, GPK2, GPK3 and GPK4, which are more than 5,000 m deep. The ultrasonic borehole imager (UBI) logs performed in the wells have revealed the presence of local damage around the wells. It results in breakouts and/or drilling-induced tensile fractures (figure 2). Depending on the depth, it appears that one damage type is predominant. An example from Valley and Evans (2006) for the well GPK3 is given on the figure 3a and b. The breakouts occur primarily below 3,000 m while the induced tensile fractures mainly appear above this depth. Most of the breakouts develop along the east-west axis. The breakouts have mechanical origin and are associated with the drilling process in an anisotropic stress context: in the simple case of a vertical borehole penetrating a rock mass in which one principal stress is vertical, breakouts indicate the orientation of the minimal horizontal stress (Bell and Gough, 1979). However, locally north-south-oriented breakouts appear (Figure 3c), *i.e.* in the direction of the major horizontal stress. According to Bérard (2003), this kind of breakout could be of thermal origin: a stable stage of pervasive tensile micro-cracking may occur before failure localizes and the resulting damage may take the shape of breakout.

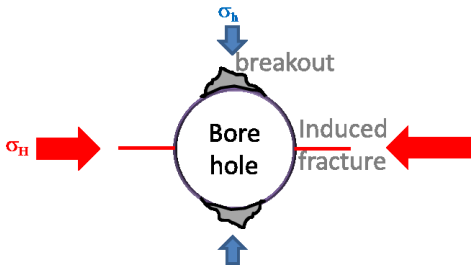

Figure 2: Schematic cross-section of a wellbore showing breakouts and induced fractures (σ_H: major horizontal stress, σ_h minor horizontal stress).

In order to study the development of near well rock mass damaging, and the conditions under which the mechanical and thermal damaging occurs, we propose to model the mechanical effect related to drilling followed by the thermo-mechanical effects induced by cold fluid injection without overpressure (case of cooling by mud during the drilling or of cooling by fluid during injection following the drilling) and with overpressure (case of development of the well). A parametric study on the difference of temperature between the rock and the injected fluid and on the applied overpressure is performed.

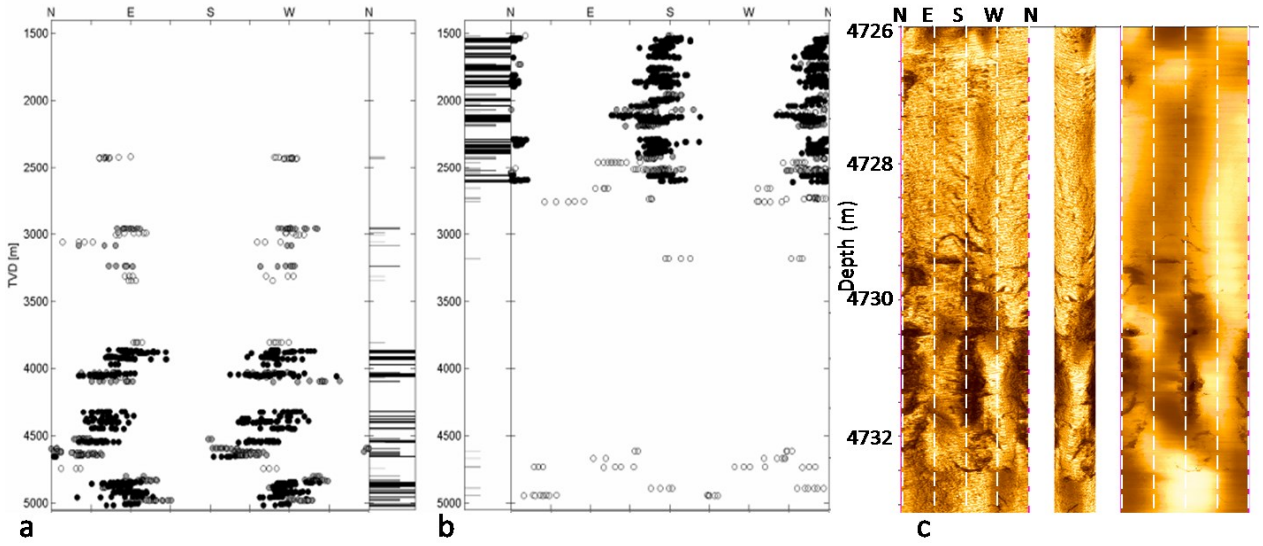

Figure 3: Orientation of breakouts (a) and drilling-induced tensile fractures (b) observed in GPK3 (Valley and Evans, 2006); c: UBI in GPK3 between 4,726 m and 4,733 m depth: breakout oriented NS.

3.2.1 Model definition

The model geometry is a 2D horizontal section of the hydrothermally altered granite centered around the vertical well. To compare the results of the modeling with the observations performed by Valley and Evans (2006) and Bérard (2003), two depths are considered: 2,000 m, where induced tensile fractures are mainly observed, and 5,000 m where breakouts are dominant. The magnitudes of major stresses are calculated from Valley and Evans (2006) characterizations of stress magnitudes.

As the DEM is very CPU time and memory size consuming, the number of needed particles of the models is limited. However, the boundaries of the model must be far enough to avoid boundary effects. That's why we chose to embed the granular near-well model (PFC) within a continuous model (FLAC, Itasca, 2002). The coupling method between the continuous and discontinuous models is developed in Shiu et al. (2011). For a well diameter of 21.6 cm, the bonded particle model size is a square of 0.65x0.65 m included in a continuous model FLAC2D of 2x2 m.

The modeling of the drilling effect is performed in two main steps. First, the stress state measured or calculated at the depth of the near well model is applied on the intact rock mass model (no well). It represents the initial state of the rock mass. Then, the mechanical effects of the well drilling are modeled by removing the particles located on the well perimeter. In order to reproduce the progressive discharge of the well linked to mud presence, a force reduction procedure is used at this step to release progressively the unbalanced force of particles lying on the well surface (Shiu et al., 2011).

The thermo-mechanical effects due to rock cooling either during the drilling process (cooling by mud injection) or during fluid injection following the drilling are studied by applying a very low over-pressure (0.1 MPa) and a heat flux corresponding to various temperature differences between fluid and rock on the particles forming the well wall (table 7). The thermo-mechanical effects of the rock cooling associated with an overpressure is modeled to study the impact of the well development on the near well rock. The over-pressure linked to the fluid injection is applied on the well boundary (5 MPa, 10 MPa and/or 15 MPa). Then, the thermal loading due to the colder fluid injection is modeled (table 7).

Initial state		Rock			Hydrothermally altered granite			
		Depth		m	2,000		5,000	
		Major horizontal stress magnitude σ_H		MPa	48		123	
		Minor horizontal stress magnitude σ_h		MPa	26		68	
		Vertical stress magnitude σ_v		MPa	52		128	
Well drilling		Discharge	Well diameter	inch	8.5		8.5	
				cm	21.6		21.6	
➥	Well cooling	Fluid overpressure		MPa	0.1		0.1	
		mud/rock temperature difference		°C	80/100/120		100/150	
➥	Well development	Fluid overpressure		MPa	5	10	10	15
		fluid/rock temperature difference		°C	80/120	80/100/120	150	100/150

Table 7: **Cases of the parametric study of the development of near well rock mass damaging at Soultz due to well drilling and to well development. Two depths are considered (2,000 m and 5,000 m) – stress magnitudes are calculated from Valley and Evans (2006).**

3.2.2 Results

Numerical results for the rock mass discharge following the well drilling are shown in Figure 4. PB cracks highlight the damage of the near well rock mass. The damage intensity is closely linked to the depth: barely no damage is observed at 2,000 m depth (only few cracks - figure 4a) whereas numerous cracks appear at 5,000 m depth (figure 4b) mainly concentrated in the direction of minor horizontal stress, and induce a changing of the well outline (figure 4c). In fact, at 5,000 m deep, the coalescence of the cracks leads to a local increase in the well radius from 10.8 cm initially to a maximum of 14.0 cm (30% increase). Beyond this increase of the well radius (interpreted as breakouts), preferably aligned cracks highlight the presence of a damaged area.

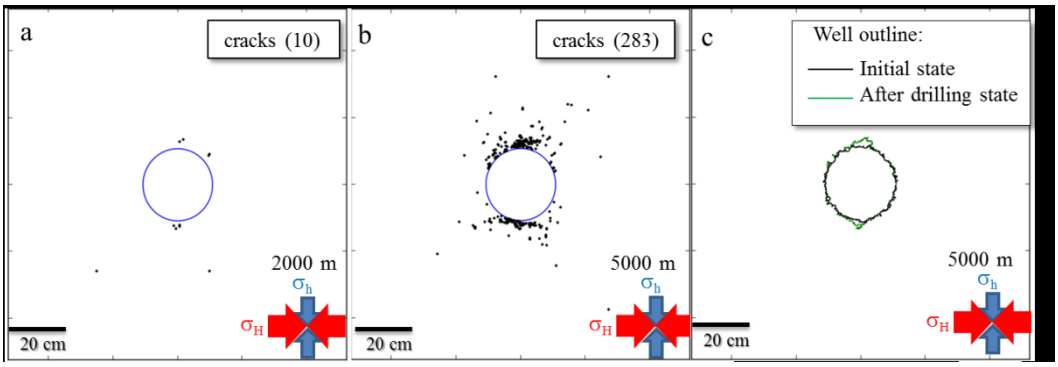

Figure 4: Cracks in the hydrothermally altered granite following the well drilling-induced discharge at 2,000 m deep (a) and at 5,000 m deep (b). c: Change in the well outline at 5,000 m resulting from the cracks coalescence.

The results of the thermo-mechanical effects due to rock cooling either during the drilling process (cooling by mud injection) or during fluid injection at 2,000 m and 5,000 m depths are shown in figure 5 and figure 6, respectively. Cooling of the rock at 80°C and 100°C generates little damage at 2,000 m deep (figure 5). A 120°C temperature difference is necessary to observe the development of thermo-mechanically induced tensile fractures in the direction of the maximum horizontal stress. The development of the main induced tensile fractures (in the direction of the major horizontal stress, figure 5A on zoomed view) is associated to the initiation of secondary tensile fractures close to the well (figure 5B on zoomed view). The propagation of these secondary fractures starts at the beginning of the thermal loading but stops at an early stage of the simulation (before 1 minute of simulated time). At a depth of 5,000 m, the thermal loading generates diffuse cracks around the well mainly in the minor horizontal stress direction.

Numerical results of the well development are shown in figure 5 (2,000 m depth) and figure 6 (5,000 m depth). At 2,000 m deep, we can observe (figure 5):

- An increasing number of the diffused cracks around the well with the increase of temperature difference and overpressure;
- The coalescence of cracks from the well wall in the direction of the major horizontal stress. It results in an initiation of induced tensile fractures for:
    - A 120°C temperature difference between the rock mass and the fluid with an overpressure of 5 MPa,
    - A 100°C temperature difference between the rock mass and the fluid with an overpressure of 10 MPa;
- As in the cooling by the mud case study, secondary tensile fractures initiation is observed (figure 5B on zoomed views); their development is quickly aborted (before 20 minutes of simulated time).

At 5,000 m depth, we can observe (figure 6):

- A number of the diffused cracks more important around the well than at a 2,000 m depth;
- For a 150°C temperature difference, the coalescence of cracks from the well wall in the direction of the major horizontal stress results in an initiation of induced tensile fractures. The fractures propagation stops before 2 minutes of thermal simulation.

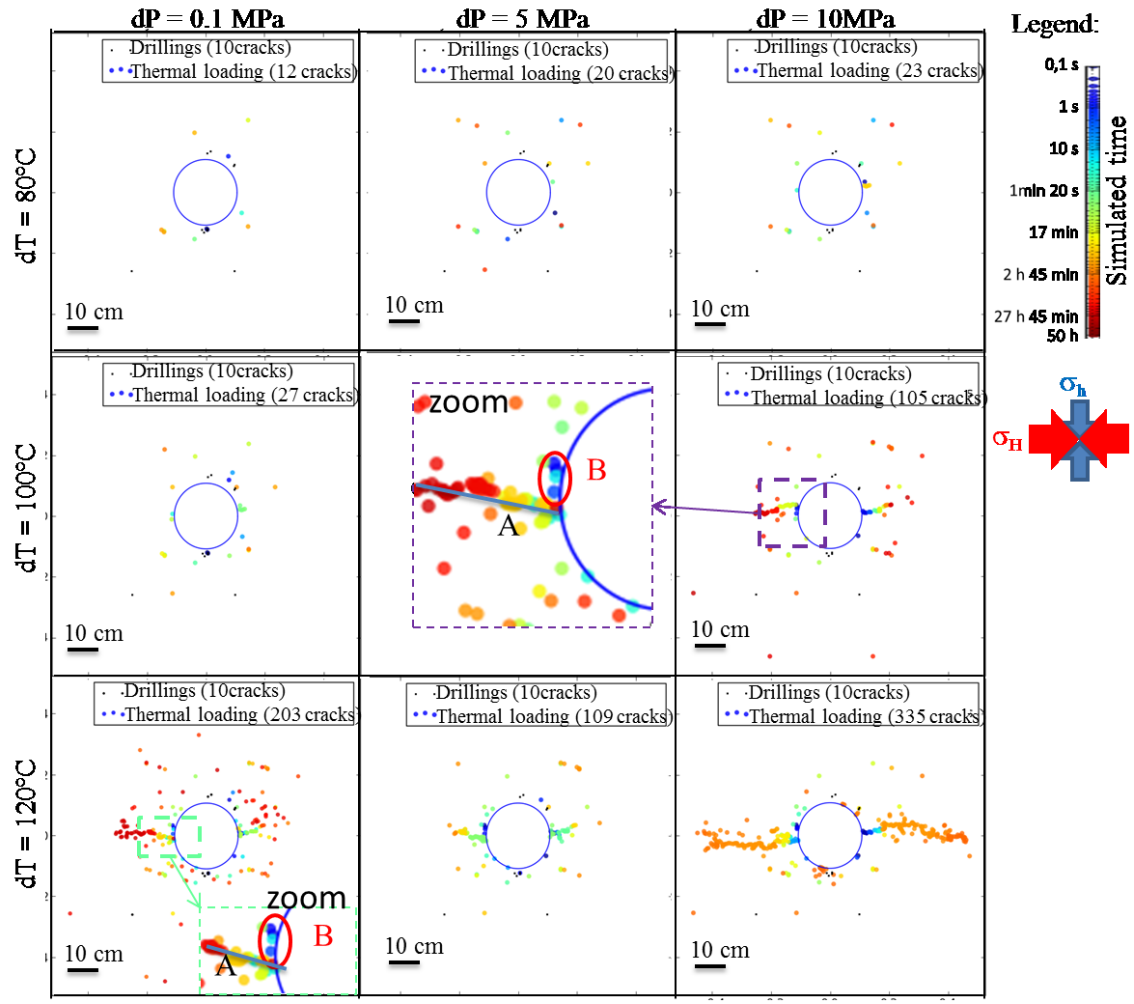

Figure 5: Simulated cracks in the hydrothermally altered granite resulting from the thermal loading at 2,000 m deep. On the zoomed views, A refers to the main tensile fracture and B to aborted tensile fractures developed from the wall of the well.

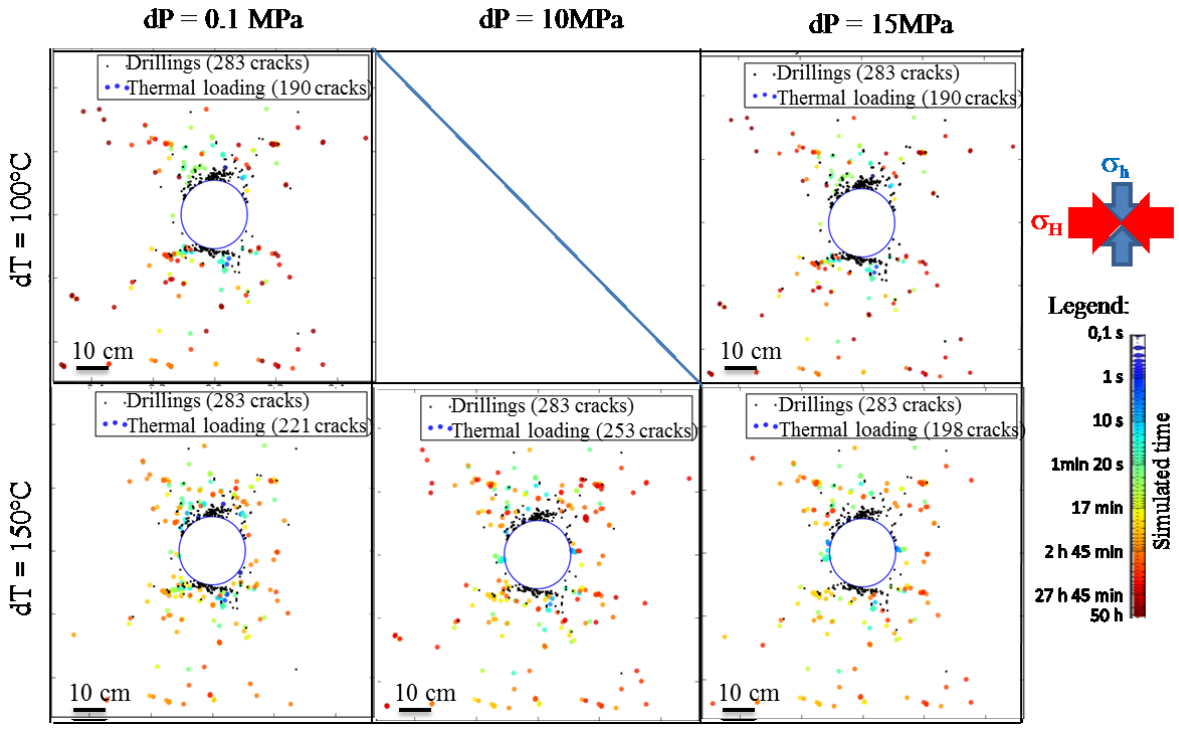

Figure 6: Simulated cracks in the hydrothermally altered granite resulting from the thermal loading at 5,000 m deep.

Globally, simulating drilling of the well highlights the formation of breakouts at a 5,000 m depth, whereas only few cracks are observed at a 2,000 m depth. The tensile fractures develop under thermal loading at 2,000 m depth and their initiation and development is facilitated by the fluid overpressure: the higher the overpressure, the lower the temperature difference required to develop tensile fractures. These results are consistent with the observations performed by Valley an Evans (2006) on UBI images in the wells. Moreover, the initiation of several tensile fractures around the well can be the source of rock ruptures that may take the shape of breakouts as suggested by Bérard (2003). The results also highlight the rock damaged zones beyond the breakouts, which can thus be taken into account in the subsequent thermal loading.

3.3 Exploitation of the well: case of Melleray

In the early 1980s, one of the first sites to exploit the deep Triassic aquifer in the Bassin de Paris (France) was set up in Melleray (Loiret). However, a significant and rapid decrease of the injectivity rate during injection tests leads the geothermal doublet to be abandoned (Boisdet et al., 1989). It was associated with a large sanding phenomenon in the injection well (partially filled with 11 m of sand). A numerical model is proposed to investigate for a potential rock damaging that can lead to a sand production. The well drilling and the first hours of its exploitation are modeled.

3.3.1 Model definition

The model is similar to that presented in section 3.2.1 for the Soultz case. The model geometry is a 2x2 m rock mass horizontal section, with the near well region (0.54x0.54 m) being modeled using the discontinuous code PFC2D and being embedded in a continuous code (FLAC2D). The considered depth corresponds to the mean depth of the injection well open-hole, *i.e.*, 1,500 m, where the rock temperature is estimated to be equal to 80°C (from Dewertz et al., 1981). A parametric study is conducted to estimate the ultimate sandstone brittleness that would correspond to the onset of sanding. Three models of sandstone, called G2, G2a and G2b from strongest to the weakest, have been built to create different levels of sandstone strength under shear and tensile stresses.

The initial stress state is assumed to be anisotropic: $\sigma_H=\sigma_v/1.4$ and $\sigma_h=\sigma_H/1.25= \sigma_v/1.75$. The principal vertical stress σ_v is taken as the overburden weight, where an average density of 2.6 is considered. The pore pressure at 1,500 m is set equal to 15 MPa (hydrostatic pressure). These assumptions lead to the following effective stress state: an effective vertical stress magnitude of 24 MPa, an effective major horizontal stress magnitude of 13 MPa, and an effective minor horizontal stress magnitude of 7 MPa.

The discharge resulting from the drilling of the 18-cm diameter well is modeled in the first place. Then, the colder temperature (35°C; BRGM, 1983) is applied on the well boundary (no overpressure is applied). Given the fine-grained structure of the sandstone, a large amount of particles has to be considered in the numerical model. To spare computational time, a one-way coupling only is taken into account to capture the effect of temperature on the mechanical behavior: a homogeneous analytical solution gives the temperature fields, which are then patched on the numerical model particles.

3.3.2 Results

The results of the mechanical effect due to the 18-cm diameter well drilling in the three sandstone models are shown in figure 7. Two different behavior of the near well rock mass are observed. The sandstones G2 and G2a, characterized by the highest strengths, are slightly damaged (figure 7a and b) whereas the important damaging of the sandstone G2b (figure 7c) leads to a local increase of the well radius in the direction of the minor horizontal stress (breakout formation): initially equal to 9 cm, it can locally reach 10.4 cm (figure 7d).

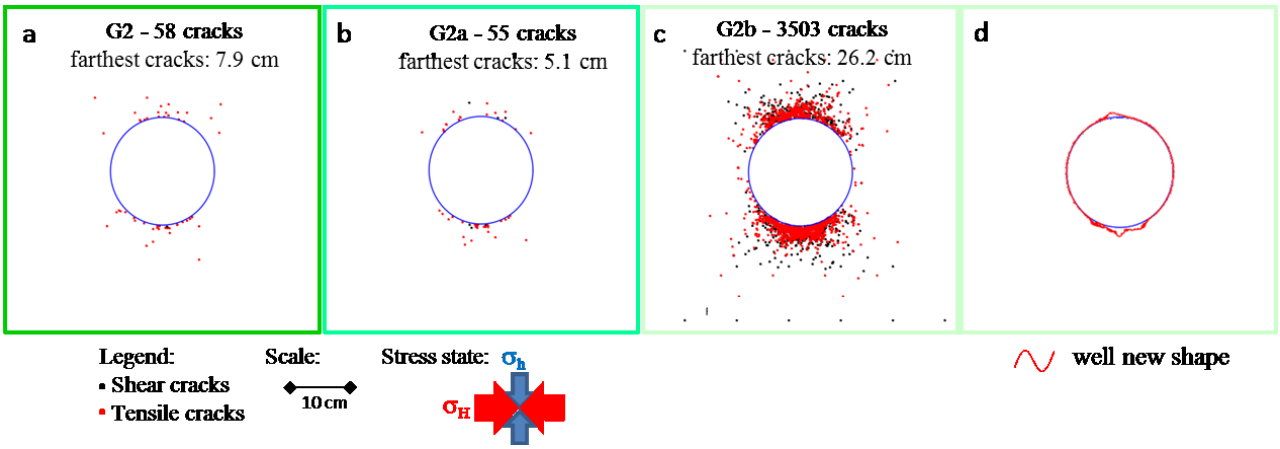

Figure 7: Simulated cracks in the sandstones resulting from the well drilling (a: G2, b: G2a, c1: G2b). d. Change in the well outline from the cracks coalescence for the model G2b.

Results of the thermal loading after first six hours of exploitation are plotted in figure 8. As for the drilling results, two behaviors are observed. On the one hand, G2 and G2a have similar damaging: a slight diffuse damaging in the direction of the minimum horizontal stress initiated at the early stage of thermal loading and associated with the development of thermo-mechanical induced tensile fractures. On the other hand, G2b has the most important damaging in the direction of the minimal horizontal stress expressed by numerous and pervasive cracks in this area. In the direction of the maximal horizontal stress, a thermo-mechanical induced tensile fracture similar to those observed for G2 and G2b is initiated. For the three sandstones, as observed in the case of Soultz, the development of the main induced tensile fractures (in the direction of the major horizontal stress, see figure 8A on zoomed view) is associated to the initiation of secondary tensile fractures close to the well (figure 8B on zoomed view).

A statistical analysis performed on the cracks that appeared during both the drilling and thermal phases highlight that PB representing grain-dolomitic cements-grain preferably break, although the clayey cement are the weakest. Further investigation should be done to understand this observation. However, this result is consistent with the *in situ* observations (BRGM, 1983): the analysis of the sand deposed in the well reveals that dolomite is frequent while clay is qualified as a trace element.

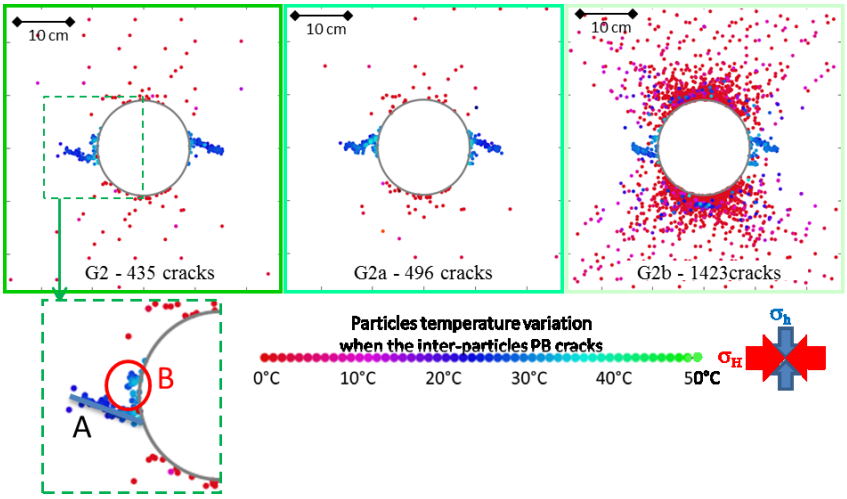

Figure 8: Simulated cracks in the sandstones after 6 hours of thermal loading over-imposed to cracks due to drilling process. A and B on zoomed view: A is the major tensile fracture and B localizes secondary aborted tensile fractures

The observed sanding process is only potentially reproduced by the weaker bonded particle sandstone model. A very low cohesion of the sandstone could produce breakout, associated with sand release in the well, given the stress state of Melleray well. The breakout formation is associated with an important diffuse damaging of the rock. We can make the assumption that this damaged rock area may be mobilized the force linked to the potential water circulation in this rock (not taken into account in the presented model). The thermal loading increases the breakout size and the diffuse rock damaging. Moreover, the tensile micro-cracking observed in the direction of the maximal horizontal stress may result in damage that takes the shape of breakout and leads to sand release in the well.

4. DISCUSSION AND CONCLUSION

In this paper, we study the effects of the mechanical and thermo-mechanical loadings due to the different processes involved in the life of a geothermal well, from drilling to exploitation, through a numerical modeling using a micro-macro approach (bonded particle models). The study is based on two real cases. The study of the drilling and the development of the well is performed on the base of the granitic reservoir of Soultz-sous-Forêts (France) and the study of the well exploitation is performed for a sandstone in the conventional heat exploitation of Melleray (Loiret, France).

In addition to being a relevant approach for thermo-mechanical processes study, the bonded particle models at grain scale allow the integration of the rock petrofabric specificity. Sandstone and granite, which are globally composed by the same mineral phases, result from different petrofabric process. As a consequence, they have very different mechanical properties. The grain size and mainly the contact properties that take into account the bond type of the rock allow the building of different mechanical behavior with similar particles properties. In the numerical models, the bonds specificities have an impact in the cracks apparition and propagation. In the case of the sandstone, we can notice that the dolomitic cements were more likely to break than the other kinds of cement. This kind of observation can be the base for a detailed petrographic study of the nature of mineral released in the well. But to validate the interpretations from this modeling, the setting of the mechanical and thermo-mechanical properties of the particles and bonds should be performed with a great care in accordance with the modeled rock element.

In both the studied cases (Soultz and Melleray), modeling at grains scale allows to reproduce the damage highlighted in the wells by direct (sand particles) or indirect (UBI) observations. The drilling process generates breakout initiation in the direction of the minimum horizontal stress. But the depth at which this phenomenon occurs depends on the stress state and the rock compressive strength (the lesser the rock compressive strength is, the shallower the breakout appears). In addition, the modeling allows the quantification of the damaging beyond the area where the rock failed. Thus, the diffuse damage developed beyond the breakout can be taken into account when the subsequent thermal loading is applied. The thermal loading associated with a large enough temperature difference and without any fluid overpressure (during drilling process or well exploitation) induces the development of thermo-mechanical tensile fractures in the direction of the maximum horizontal stress. The development of the main induced tensile fractures is sometimes associated to the initiation of secondary tensile fractures close to the well. The propagation of these secondary fractures starts at the beginning of the thermal loading but stops at an early stage of the modeling. These tensile fractures may result in rock ruptures that may take the shape of breakouts (thermal breakouts) as suggested by Bérard (2003). During the simulation of well development, the overpressure applied at the well wall makes the tensile fractures propagation easier. It may enhance and accelerate the rock mass damage linked to the thermal loading initiated during the well drilling in the direction of the maximal horizontal stress.

These simulations highlight the thermo-mechanical damage of a geothermal well linked to the different steps of its life. The analytical solution cannot take into account all the complexity of the processes and the pre-damaging of the rock. In perspective of this work, we plan to take into account all the history of the well to have a complete overview of the damage resulting from the

superimposition of the different steps: drilling, cooling by the mud, cooling by fluid injection (injection test) with or without overpressure, cooling and overpressure apply during well development if needed, and finally well exploitation.

ACKNOWLEDGEMENT

This research was carried out in the framework of both the GEISER (Geothermal Engineering Integrating Mitigation of Induced Seismicity in Reservoirs) European project funded by the European Commission and the CLASTIQ2 project funded by the BRGM and the French Environment and Energy Management Agency. The authors are grateful to Fabian Dedecker and Wenjie Shiu from Itasca Consultants S.A.S. for technical support for these modeling.

REFERENCES

Bell J.S. and Gough D.I., 1979, Northeast-southwest compressive stress in Alberta evidence from oil wells, Earth and Planetary Science Letters, 45, pp.475-482

Bérard Th., 2003, Estimation du champ de contrainte dans le massif granitique de Soultz-sous-Forêts : implication sur la rhéologie de la croûte fragile. Thèse de Doctorat, IPGP, 266 p.

Boisdet A., Cautru J.-P., Czernichowski-Lauriol I., Detoc S., Fouchet J.-L., Fouillac C., Honegger J.-L., Martin J.-C., Vuataz F.-D., 1989, Projet Trias : expérimentation en vue de la réinjection de saumures géothermales dans les grès du Trias profond, Rapport 89-SGN-141 3E/IRG, 110 p.

BRGM, 1983, Forage géothermique de Melleray (GMY2) : essais de contrôle des caractéristiques du puits d'injection réalisés en mai et juin 1982, rapport 83-SGN-176-GTH, 95 p.

Cautru.J.P., and Robelin.C, 1984, Etude d'un réservoir argilo-gréseux - cas du Trias du doublet géothermique de Melleray (Loiret). Lithologie, corrélations faciologiques et diagraphiques -première approche pétrographique de la réinjection-Rapport 84, SGN, 124, IRG

Cundall PA., 1971, A computer model for simulating progressive largescale movements in blocky rock systems. In: Proceedings of the Symposium of International Society of Rock Mechanics, vol. 1, Nancy: France; 1971. Paper No. II-8.

Dewertz A., Herbrich B., Fabris H., Maget Ph., Menjoz A., Tournaye D., 1981, GMY2 Forage géothermique de Melleray, réinjection, 76 p.

Gentier S., Genter A., Bourgine B., Chilès J.P., Delpont G., Riss J., Billaux D., Dedecker F., Bruel D., 2002. Modélisation de l'interface puits-échangeur (site de Soultz-sous-Forêts). Acquisition de données de base et développements préliminaires, Report BRGM/RP 51764-FR, 349 p.

Itasca Consulting Group, Inc., 2002, 4.0th ed. Fast lagrangian analysis of continua, 4.0 Minneapolis: Itasca.

Itasca Consulting Group, Inc., 2008a, PFC2D – Particle Flow Code in 2 Dimensions, Ver. 4.0, Theory and Background Manual. Minneapolis: Itasca.

Itasca Consulting Group, Inc., 2008b, PFC2D – Particle Flow Code in 2 Dimensions, Ver. 4.0, Optional Features Manual. Minneapolis: Itasca.

Morita N. and Boyd P.A., 1991, Typical Sand Production Problems: Case Studies and Strategies for Sand Control, Paper SPE 22739 presented at the 66th Annual Technical Conference and Exhibition of the Society of Petroleum Engineers held in Dallas, TX, October 5-9, 1991.

Peter-Borie M., Blaisonneau A., Gentier S., Rachez X., Shiu W., Dedecker F., 2011, A particulate rock model to simulate thermo-mechanical cracks induced in the near well by supercritical CO_2 injection, Proceedings of the Congress Mathematical Geosciences at the crossroads of theory and practice, Int. Assoc. for Mathematical Geology, September 5th-9th, 2011, Salzburg, Austria, 15 p.

Peter-Borie M., Gentier S., Blaisonneau A., Guillon T., Rachez X., 2014, De la roche à son modèle numérique par approche particulaire : conceptualisation et applications, JNGG 2014, Beauvais, les 8, 9 et 10 juillet 2014, 10 p.

Potyondy, D.O. and Cundall, P.A., 2004, A Bonded-Particle Model for Rock. Int. J. Rock Mech. & Min. Sci. 41(8), 1329-1364.

Riss, J., Gentier, S., Genter, A. 2001. Granitic core cross section: numerical modelling. In Proceedings of the 8th International Symposium for Stereology and Image analyses, 6 p.

Shiu W.J., F. Dedecker, X. Rachez, M. Peter-Borie, 2011, Discrete modeling of near-well thermo-mechanical behavior during CO_2 injection, Proceedings of the 2nd International FLAC/DEM Symposium, February 14th-16th, 2011, Melbourne, Australia, 8p.

Stephens G and Voight B., 1982, Hydraulic Fracturing Theory for Conditions of Thermal Stress, Int. d. Rock Mech. Min. Sci. & Geomech. Ahstr. Vol. 19, pp. 279:284

Valley B. and Evans K.F., 2006, Stress state at Soultz to 5km depth from wellbore failure and hydraulic observations. EHDRA meeting June 2006, Soultz-sous-Forêts, 15 p.

Wanne T.S. and Young R.P., 2008, Bonded-particle modeling of thermally fractured granite, International Journal of Rock Mechanics & Mining Sciences 45, pp. 789–799.

Zoback M. D.,Moos, D. Mastin L., 1985, Well Bore Breakouts and in Situ Stress, Journal Of Geophysical Research, Vol. 90, No. B7, June 10, pp. 5523-5530.